Upper ocean carbon export, horizontal transport, and vertical eddy diffusivity in the southwestern Gulf of Maine

Claudia R. Benitez-Nelson*, Ken O. Buesseler, Glenn Crossin

Department of Marine Chemistry and Geochemistry, Woods Hole Oceanographic Institution, 226 Woods Hole Road, Woods Hole, MA 02543, USA

Abstract

The naturally occurring radionuclides ^{234}Th and ^{7}Be were used to investigate the magnitude of upper ocean particulate organic carbon export and the rate of vertical eddy diffusion in the southwestern Gulf of Maine. Sampling occurred during the spring (March, April) and summer (July, August) of 1997. Both non-steady-state and horizontal transport models were assessed and found to be very important for the accurate determination of ^{234}Th export. Upper ocean particulate organic carbon export was estimated using modeled ^{234}Th export and the ratio of particulate organic carbon to ^{234}Th on GF/F filters. Our measurements demonstrate that the southwestern Gulf of Maine is typical of many coastal regimes, having an organic carbon export ratio (particulate export/primary production) which ranges from 9 to 49% depending on the depth of integration and primary productivity estimate. ^{7}Be derived estimates of vertical eddy diffusivity into summer surface waters ranged from 0.5 to 1.5 cm^2 sec^{-1}, and show that this mechanism is sufficient to support the amount of 'new' nitrogen required for the measured particulate carbon export. © 2000 Elsevier Science Ltd. All rights reserved.

Keywords: Carbon export; Thorium; Beryllium; Vertical eddy diffusion; Regional index term; USA; New England; Gulf of Maine

1. Introduction

Coastal environments have long been known to play a disproportionate role in total oceanic primary production and particulate organic carbon export (Eppley and

---

*Corresponding author. Present address: Department of Oceanography, University of Hawai'i, MSB 610, 1000 Pope Road, Honolulu, HI 96822, USA. Tel.: (808) 956-7625; fax: (808) 956-9516.

E-mail address: cbnelson@soest.hawaii.edu (C.R. Benitez-Nelson)

Peterson, 1978). However, the temporal and spatial variability of these processes remains vague. Knowledge of particulate export has proven to be essential for predicting the fate of organically bound or biologically active contaminants, such as anthropogenically produced CO_2, hydrocarbons and heavy metals (Wageman and Muir, 1984; Larsen et al., 1985; Barrick and Prahl, 1987; US JGOFS Rept. 11, 1990; Kennicutt et al., 1994). Recently developed techniques to investigate particulate removal in the open ocean utilizes the disequilibrium between particle reactive ^{234}Th ($t_{\frac{1}{2}} = 24.1$ d) and its conservative long-lived parent, ^{238}U ($t_{\frac{1}{2}} = 4.5 \times 10^9$ y) (Coale and Bruland, 1985, 1987; Murray et al., 1989; Buesseler et al., 1992a, 1998; Bacon et al., 1996; Murray et al., 1996). Yet, there have been few studies which have used this measurement in a coastal environment (Wei and Murray, 1992; Cochran et al., 1995; Gustafsson et al., 1998).

In this paper, we have used ^{234}Th to elucidate particulate organic carbon export rates in the southwestern Gulf of Maine. The Gulf of Maine is a highly productive continental shelf sea situated along the northeastern coast of the United States and southwestern Nova Scotia. Within the Gulf, there are three major deep (>275 m) basins, Jordan, Wilkinson, and Georges, which are separated at the ~ 200 m isobath by various topographic rises and banks (Brooks, 1991). This semi-enclosed water mass is bordered by a heavily populated coastline and supports one of the largest fisheries industries in North America (O'Reilly and Busch, 1984). Unfortunately, increasing anthropogenic inputs from agricultural and industrial activities have placed this unique basin in jeopardy.

There are currently few direct measurements of particulate export in the Gulf of Maine (Moran and Buesseler, 1993; Charette et al., 1996, 2000). Primary production within the region is known to vary seasonally (O'Reilly and Busch, 1984). In winter, deep convective mixing (100–200 m), limits the light available for phytoplankton growth (Sverdrup, 1953; Townsend and Spinrad, 1986). In spring, the onset of thermal stratification initiates a spring bloom dominated by large, rapidly growing primary producers such as diatoms (O'Reilly and Busch, 1984; Townsend and Spinrad, 1986). The presence of these large organisms appears to be directly related to high particulate export rates in the upper ocean (Buesseler, 1998). Strong thermal stratification and nutrient depletion ($NO_3 + NO_2 \approx 0$) in the summer reduces biomass, resulting in a change in food web structure to smaller phytoplankton and bacteria, which are more efficient at nutrient uptake and remineralization (Walsh et al., 1987). A second period of high particulate export may occur in mid to late summer as result of fecal pellet production and grazing of dense populations of copepods (e.g. Meise and O'Reilly, 1996).

The particulate carbon export that results from this seasonally changing community structure is unknown. Within the Gulf of Maine, there are a wide range of estimates of new and recycled production, of which many are inferred from limited data sets (O'Reilly and Busch, 1984; Campbell, 1986; Schlitz and Cohen, 1984; Townsend, 1991, 1998; Christensen et al., 1991). In a recent study, Townsend (1998) determined that the total flux of 'new' nitrogen into the Gulf of Maine, i.e. that which supports 'new production', corresponded to 13.5 mmol C m^{-2} d^{-1}. When compared to estimated rates of total primary production of 66.2 mmol C m^{-2} d^{-1} (O'Reilly and

Busch, 1984), an average export ratio (export versus total production) of 0.20 can be determined. Townsend (1998), however, hypothesized that the actual export ratio was closer to 0.40 based on what had been found in other coastal environments. As a result, Townsend (1998) suggested that another possible source of new nitrogen to surface waters is via water column nitrification followed by upward diffusion *within* the Gulf of Maine. Unfortunately, there was little direct evidence to support this conclusion.

In this study, we examined the magnitude of particulate carbon export using ^{234}Th over the spring (March and April) and summer (July and August) of 1997 in the southwestern Gulf of Maine. Both non-steady-state and horizontal models were evaluated. In addition, upper ocean vertical eddy diffusivity rates were measured using ^{7}Be.

2. Methods

Samples were collected during four cruises in the spring and summer of 1997 in Wilkinson Basin (depth = 280 m) in the Gulf of Maine. Sample locations are provided in Table 1, and are shown in Figs. 1 and 2. This particular basin was chosen due to its relatively low advection and diffusion rates (Vermersch et al., 1979; Brooks, 1985) and its close proximity to the Woods Hole Oceanographic Institution. Cruises were conducted in two paired sets, March and April, and July and August. A suite of surface samples and one depth profile (st. 7 in all cruises) were collected. A large diameter hose was placed over the side of the ship and water pumped on deck using a rotary bronze gear pump (Model: Teel, $\frac{1}{4}$ port). For ^{234}Th and ^{7}Be, between 200 and 400 L of seawater were passed sequentially through a 1 μm polypropylene Hytrex filter followed by two 3 inch MnO_2-impregnated Hytrex cartridges and a 1 L PVC pipe packed with iron-impregnated polypropylene sheets. A flowmeter was placed on the end of the PVC pipe in order to monitor flow rate and volume. MnO_2 adsorbers have been previously shown to efficiently collect dissolved ^{234}Th (Buesseler et al., 1992b, 1995). The activity of ^{234}Th can be quantified by determining the MnO_2 collection efficiency from:

Collection efficiency $= 1 - B/A$

where A and B are the ^{234}Th activities in disintegrations per minute (d.p.m.) on the first and second MnO_2 cartridges in the series. ^{234}Th collection efficiencies averaged 0.86 ± 0.08 ($n = 66$).

While the MnO_2 cartridges collect ^{234}Th, they have poor collection efficiencies for ^{7}Be. Tests conducted by this laboratory found that less than 5% of the dissolved ^{7}Be activity was collected on both the Mn A and Mn B ^{234}Th cartridges. In contrast, previous investigations have found that ^{7}Be is efficiently collected using iron oxide-impregnated materials (Lee et al., 1991; Luo et al., 1995). Although ^{234}Th can also be collected using iron oxide, our tests found that variable amounts of the parent radionuclide, ^{238}U, were adsorbed as well. Inconsistent adsorption of ^{238}U will result in variable ingrowth of ^{234}Th with time, compromising the ^{234}Th data. Thus, two

Table 1
Radionuclide data from samples collected in the southwestern Gulf of Maine. All data, with the exception of station 7 depth profiles, were collected at 5 m. Error bars are 1σ. B.D. = Below Detection

Station	Lat. (N)	Long. (W)	Part. ^{7}Be (d.p.m. m^{-3})	Diss. ^{7}Be (d.p.m. m^{-3})	Part. ^{234}Th (d.p.m. L^{-1})	Diss. ^{234}Th (d.p.m. L^{-1})	POC/^{234}Th (μmol d.p.m.$^{-1}$)
March 1997							
1	42°30.0	70°29.9	7.8 ± 8.4	373 ± 28	0.24 ± 0.02	0.40 ± 0.02	58 ± 6
2	42°40.2	70°22.1	3.8 ± 7.5	109 ± 2	0.34 ± 0.02	0.49 ± 0.02	26 ± 4
3	42°51.0	70°29.8	9.6 ± 7.0	199 ± 18	0.36 ± 0.03	0.52 ± 0.02	19 ± 4
4	43°00.0	70°24.4	4.3 ± 8.7	86 ± 15	0.27 ± 0.02	0.65 ± 0.03	39 ± 5
5	42°59.7	70°12.0	4.7 ± 4.4	200 ± 22	0.49 ± 0.04	0.58 ± 0.03	17 ± 3
6	42°53.1	70°09.2	6.6 ± 9.2	247 ± 19	0.39 ± 0.02	0.61 ± 0.03	17 ± 3
7, 5 m	42°29.1	69°43.7	21.2 ± 12.6	174 ± 21	0.75 ± 0.05	0.73 ± 0.03	5 ± 2
20 m			B.D.	152 ± 16	0.44 ± 0.04	0.68 ± 0.03	7 ± 1
35 m			B.D.	93 ± 20	0.61 ± 0.06	0.79 ± 0.03	5 ± 1
50 m			0.7 ± 6.4	132 ± 13	0.25 ± 0.03	0.58 ± 0.02	22 ± 5
72 m			6.9 ± 17.7	133 ± 7	0.53 ± 0.03	0.81 ± 0.03	9 ± 2
8	42°46.0	70°18.2	6.6 ± 9.9	218 ± 22	0.35 ± 0.03	0.61 ± 0.03	17 ± 4
9	42°35.9	70°12.1	14.5 ± 19.2	171 ± 16	0.36 ± 0.03	0.67 ± 0.03	9 ± 4
April 1997							
1	42°46.0	69°43.5	19.4 ± 7.1	268 ± 12	0.41 ± 0.03	1.11 ± 0.03	60 ± 4
2	42°47.2	69°57.3	16.3 ± 5.5	495 ± 22	0.49 ± 0.02	1.17 ± 0.03	13 ± 3
3	43°01.0	69°44.8	16.2 ± 7.1	341 ± 20	0.47 ± 0.02	0.95 ± 0.03	34 ± 3
4	43°15.0	69°50.0	21.2 ± 6.5	326 ± 20	0.48 ± 0.02	1.11 ± 0.03	14 ± 3
5	42°59.8	70°12.1	26.5 ± 8.0	307 ± 18	0.40 ± 0.02	0.62 ± 0.02	24 ± 3
6	42°60.0	70°24.5	23.3 ± 6.8	305 ± 15	0.29 ± 0.02	0.71 ± 0.02	33 ± 5
7, 5 m	42°29.9	69°45.1	5.1 ± 4.9	222 ± 17	0.49 ± 0.04	1.27 ± 0.03	11 ± 3
30 m			B.D.	343 ± 30	0.45 ± 0.04	1.09 ± 0.03	15 ± 3
60 m			B.D.	320 ± 25	0.45 ± 0.03	1.13 ± 0.03	18 ± 3
90 m			30.5 ± 27.7	273 ± 19	0.12 ± 0.05	1.26 ± 0.04	44 ± 20
111 m			8.2 ± 7.3	238 ± 11	0.45 ± 0.15	1.57 ± 0.05	9 ± 5
8	42°50.6	70°29.7	23.8 ± 13.5	327 ± 30	0.34 ± 0.05	0.92 ± 0.03	32 ± 6
9	42°46.1	70°18.4	7.5 ± 17.6	210 ± 29	0.27 ± 0.04	0.92 ± 0.02	46 ± 9
10	42°35.8	70°12.0	15.0 ± 2.1	258 ± 20	0.27 ± 0.04	0.80 ± 0.02	30 ± 6
11	42°24.9	70°47.9	80.9 ± 20.0	214 ± 9	0.19 ± 0.05	0.43 ± 0.01	117 ± 29
12	42°20.7	70°23.6	B.D.	180 ± 30	0.43 ± 0.08	0.57 ± 0.01	35 ± 7
13	42°20.1	69°57.0	31.5 ± 18.8	341 ± 25	0.65 ± 0.07	2.09 ± 0.04	62 ± 7
July 1997							
1	42°44.8	69°42.5	3.9 ± 9.4	478 ± 31	0.49 ± 0.02	1.15 ± 0.03	15 ± 3
2	42°46.9	69°57.2	B.D.	245 ± 19	0.30 ± 0.02	1.20 ± 0.03	22 ± 5
3	43°15.0	69°49.9	16.2 ± 11.7	413 ± 29	0.30 ± 0.02	0.72 ± 0.02	37 ± 5
4	43°09.0	70°00.5	6.3 ± 5.6	390 ± 19	0.16 ± 0.01	0.36 ± 0.01	68 ± 10
5	43°00.1	70°24.4	B.D.	600 ± 22	0.19 ± 0.02	0.54 ± 0.01	26 ± 7
6	42°28.7	69°44.1	B.D.	479 ± 24	0.22 ± 0.01	0.91 ± 0.02	30 ± 6
7, 5 m	42°29.1	69°44.1	5.8 ± 16.3	370 ± 5	0.30 ± 0.06	1.14 ± 0.04	18 ± 5
15 m			12.7 ± 7.6	184 ± 16	0.51 ± 0.04	1.17 ± 0.03	9 ± 3
37 m			7.2 ± 3.4	92 ± 21	0.55 ± 0.04	1.26 ± 0.04	16 ± 3
50 m			B.D.	119 ± 20	0.92 ± 0.05	0.85 ± 0.03	5 ± 1

(*Table continued in next page*)

Table 1 (*Continued*)

Station	Lat. (N)	Long. (W)	Part. ^{7}Be (d.p.m. m^{-3})	Diss. ^{7}Be (d.p.m. m^{-3})	Part. ^{234}Th (d.p.m. L^{-1})	Diss. ^{234}Th (d.p.m. L^{-1})	POC/^{234}Th (μmol d.p.m.$^{-1}$)
65 m			B.D.	125 $\pm$ 16	1.29 $\pm$ 0.05	0.99 $\pm$ 0.03	2 $\pm$ 1
8	42°50.9	70°29.9	B.D.	340 $\pm$ 24	0.23 $\pm$ 0.03	0.83 $\pm$ 0.02	42 $\pm$ 8
9	42°45.8	70°17.8	1.8 $\pm$ 5.4	226 $\pm$ 20	0.26 $\pm$ 0.02	0.90 $\pm$ 0.02	20 $\pm$ 5
10	42°36.0	70°12.0	31.6 $\pm$ 21.2	504 $\pm$ 23	0.41 $\pm$ 0.04	0.95 $\pm$ 0.02	30 $\pm$ 5
11	42°33.9	70°30.1	10.7 $\pm$ 7.4	146 $\pm$ 19	0.36 $\pm$ 0.03	0.76 $\pm$ 0.02	27 $\pm$ 4
12	42°25.7	70°44.9	9.6 $\pm$ 8.8	205 $\pm$ 22	0.50 $\pm$ 0.04	0.35 $\pm$ 0.01	45 $\pm$ 4
13	42°10.5	70°23.6	B.D.	212 $\pm$ 23	0.44 $\pm$ 0.07	0.70 $\pm$ 0.02	23 $\pm$ 5
Aug 1997							
1	42°44.5	69°42.2	B.D.	436 $\pm$ 46	0.15 $\pm$ 0.04	0.80 $\pm$ 0.02	39 $\pm$ 14
2	42°47.0	69°57.0	B.D.	627 $\pm$ 51	0.40 $\pm$ 0.02	1.03 $\pm$ 0.03	16 $\pm$ 8
3	43°01.0	69°43.9	2.1 $\pm$ 4.6	541 $\pm$ 81	0.07 $\pm$ 0.03	1.54 $\pm$ 0.04	113 $\pm$ 39
4	43°15.0	69°50.1	B.D.	145 $\pm$ 45	0.13 $\pm$ 0.02	0.80 $\pm$ 0.02	131 $\pm$ 242
5	43°09.2	70°05.2	B.D.	243 $\pm$ 52	0.05 $\pm$ 0.02	0.46 $\pm$ 0.01	191 $\pm$ 79
6	42°60.0	70°24.5	B.D.	361 $\pm$ 54	0.02 $\pm$ 0.02	0.54 $\pm$ 0.01	272 $\pm$ 348
7, 5 m	42°29.5	69°42.8	B.D.	379 $\pm$ 49	0.35 $\pm$ 0.11	1.32 $\pm$ 0.03	21 $\pm$ 4
15 m			B.D.	433 $\pm$ 71	0.22 $\pm$ 0.06	1.35 $\pm$ 0.04	35 $\pm$ 24
30 m			B.D.	191 $\pm$ 63	0.11 $\pm$ 0.05	1.08 $\pm$ 0.03	83 $\pm$ 44
45 m			11.5 $\pm$ 3.5	14 $\pm$ 12	0.07 $\pm$ 0.03	1.24 $\pm$ 0.04	37 $\pm$ 39
60 m			11.3 $\pm$ 3.9	9 $\pm$ 9	0.01 $\pm$ 0.01	1.23 $\pm$ 0.04	534 $\pm$ 799
8	42°51.0	70°30.0	B.D.	393 $\pm$ 67	0.03 $\pm$ 0.04	0.63 $\pm$ 0.02	405 $\pm$ 555
9	42°46.1	70°18.0	6.8 $\pm$ 4.4	496 $\pm$ 55	0.04 $\pm$ 0.03	0.82 $\pm$ 0.03	153 $\pm$ 113
10	42°36.0	70°12.3	10.2 $\pm$ 6.7	342 $\pm$ 51	0.37 $\pm$ 0.09	0.80 $\pm$ 0.02	17 $\pm$ 5
11	42°30.0	70°30.0	B.D.	232 $\pm$ 50	0.09 $\pm$ 0.02	0.59 $\pm$ 0.02	94 $\pm$ 24
12	42°25.1	70°47.9	13.4 $\pm$ 2.8	451 $\pm$ 88	0.23 $\pm$ 0.01	0.29 $\pm$ 0.01	74 $\pm$ 6
13	42°10.6	70°23.3	B.D.	142 $\pm$ 27	0.95 $\pm$ 0.27	0.43 $\pm$ 0.02	9 $\pm$ 4

separate sets of radionuclide samples were collected: ^{7}Be on Fe(OH)$_3$ and ^{234}Th on MnO$_2$. ^{7}Be collection efficiencies were determined in the same manner as for ^{234}Th, by splitting the cartridge into an *A* and *B* section. Collection efficiencies were lower and more variable than that found with ^{234}Th and averaged 0.71 $\pm$ 0.19 ($n = 49$). Variability in ^{7}Be collection efficiencies was most likely the result of non-uniform iron impregnation of the polypropylene filters.

All ancillary samples were collected using 30 L Nisken bottles. Discrete unfiltered and filtered (through a GF/F) nutrient samples were collected in acid-cleaned polypropylene bottles and immediately frozen for analysis in the laboratory. Suspended particulate matter (SPM) samples were collected by filtering 2 L of seawater onto pre-weighed 47 mm polycarbonate filters. Particulate organic carbon and separate pigment samples were collected via low pressure (<5 psi) filtration of 2 L of seawater onto pre-combusted 25 mm GF/F filters.

Upon returning to the lab, ^{234}Th MnO$_2$ cartridges were immediately acid-digested, purified, and counted via low-level beta counting according to the methods described by Buesseler et al. (1992b). Iron oxide and Hytrex prefilters were ashed and placed in

$$^{234}Th \ (dpm \ L^{-1})$$
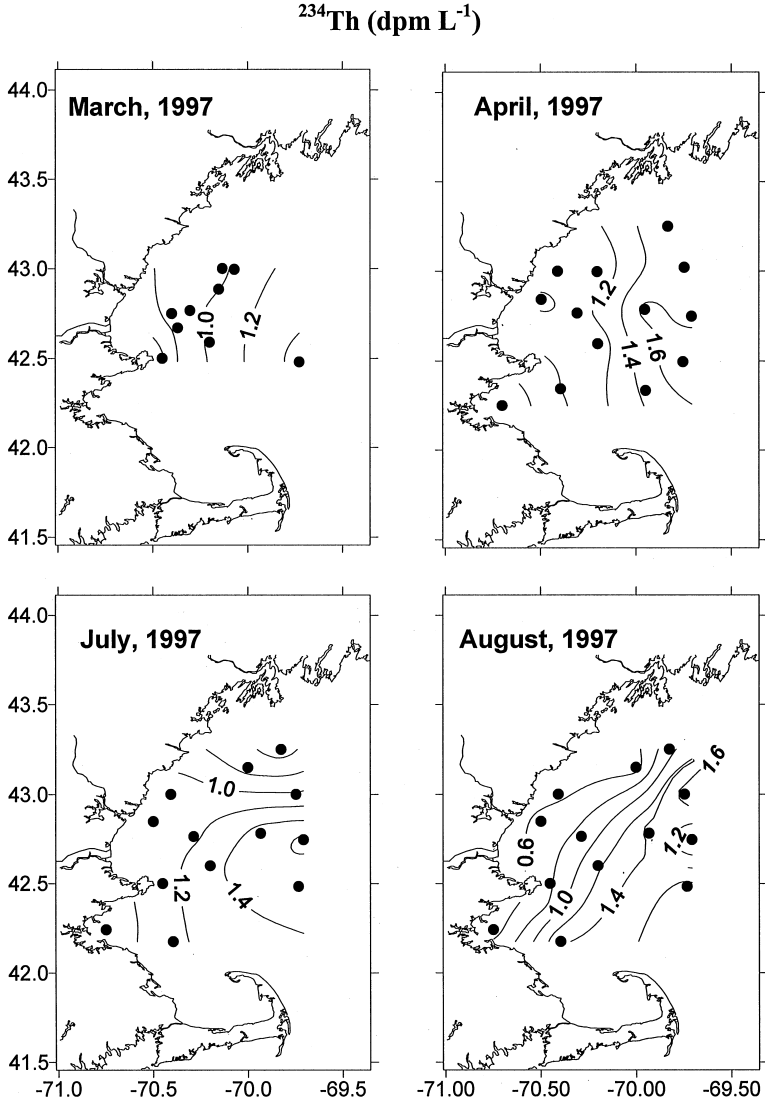
Fig. 1. (a)–(d) Contour plots of total ^{234}Th surface activities in d.p.m. L^{-1} from all four cruises. Station locations are shown as black circles.

clear pre-weighed polystyrene counting jars. Iron oxide filters were measured for ^{7}Be and Hytrex prefilters for both ^{7}Be and ^{234}Th using CANBERRA 2000 mm^2 LEGe style gamma detectors. ^{234}Th gamma ($E_n = 63$ KeV) and low-level beta efficiencies have been determined previously (Buesseler et al., 1992b, 1995). For ^{7}Be ($E_n = 477$ KeV), gamma detectors were calibrated using standards of known activity (EPA

^{7}Be (dpm m^{-3})
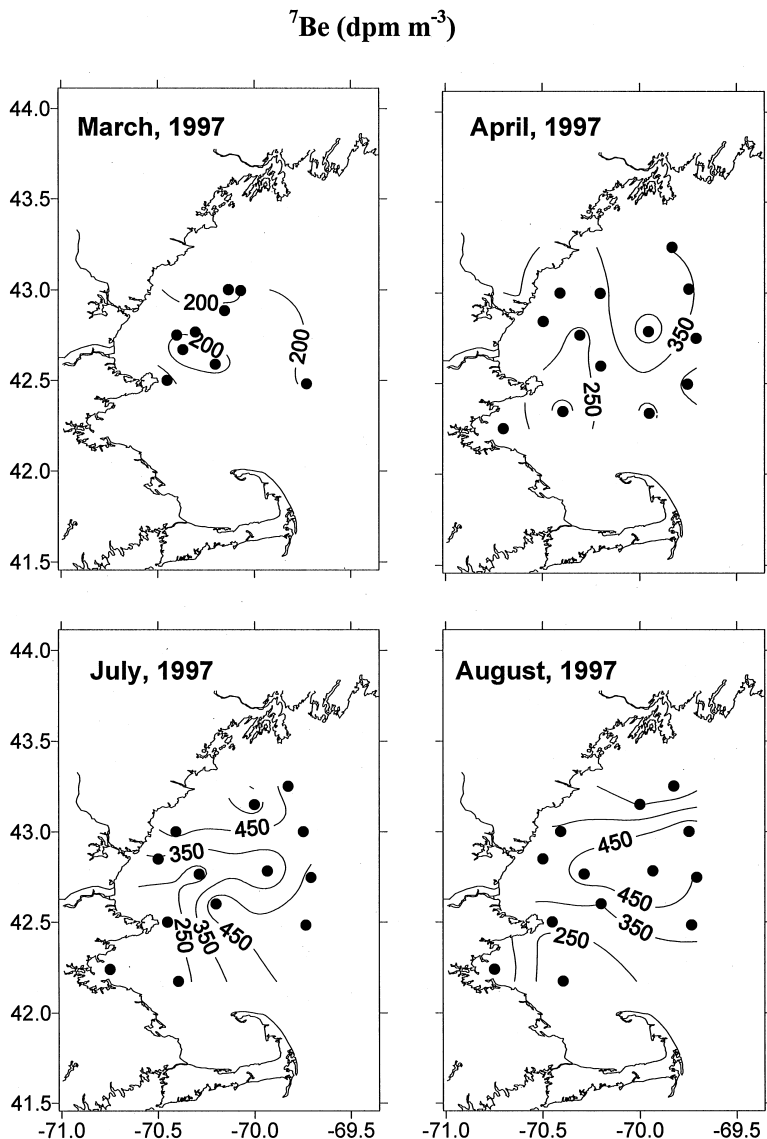
Fig. 2. (a)–(d) Contour plots of total ^{7}Be surface activities in d.p.m. m^{-3} from all four cruises. Station locations are shown as black circles.

Standard Pitchblend Ore). Standards of similar geometry and of differing heights were placed in the same counting jars used for our samples. ^{7}Be efficiencies and self-absorption were then determined by interpolating between the gamma emissions of ^{214}Pb (242, 295, 352 keV) and ^{314}Bi (609 keV). An additional check of this interpolation procedure was conducted by directly comparing the interpolated efficiencies

found for ^{137}Cs (661 keV) with those derived from counting a known activity ^{137}Cs standard. Interpolated and measured ^{137}Cs efficiencies were within 5% of each other. ^{234}Th and ^{7}Be activities were corrected to the midpoint of collection and reported in disintegrations per minute (d.p.m.). Activity errors were determined from the propagation of uncertainties derived from volume collection, detector calibration, and for ^{234}Th chemical recoveries. All errors are 1σ.

Ancillary measurements for total and dissolved ($<0.7\ \mu$m) $NO_3 + NO_2$, ammonia, silicate, and phosphorus were analyzed by the Analytical Service Center at the Virginia Institute of Marine Science according to the methods described by Pollard et al. (1996). Dissolved organic carbon measurements were made according to Peltzer and Hayward (1996). Pigments in the greater than $0.7\ \mu$m size class were determined using HPLC according to Zapata et al. (1987). Particulate organic carbon and nitrogen were determined on subsamples ($\frac{1}{4}$ of the total) of the GF/F filters using a CHN analyzer. All CHN samples were processed according to Gunderson et al. (1993), the same procedure utilized at the JGOFS Bermuda Atlantic Time Series. This method involves drying the filter subsamples in a 60°C oven followed by fuming with concentrated HCl for 24 h prior to measurement in order to remove carbonate.

3. Results

Dissolved and particulate ^{234}Th and ^{7}Be surface water activities are shown in Table 1. Total ^{234}Th and ^{7}Be surface activity distributions are shown in Figs. 1 and 2. Contour plots were constructed using a software package (SURFER™ by Golden Software), which utilizes a linear kriging technique to grid the data. Kriging is a technique that places irregularly spaced data on a regularly spaced grid. Each grid point or node is determined by an average value that is the result of weighting all of the data in accordance with their proximity to the actual grid point. In essence, the closer the data point, the higher the weighting factor in the determination of the concentration at that grid point. Station locations are shown for each cruise and grid scales are uniform to better demonstrate temporal and spatial trends in our radionuclide data.

In March, nutrients were high and the mixed layer depth at our vertical profile station (st. 7) was 100 m (Fig. 3), indicating that the spring bloom had yet to begin (Townsend and Spinrad, 1986; Durbin et al., 1995). Total surface ^{234}Th activities ranged from 0.6 to 1.5 d.p.m. L^{-1} and increased with increasing distance from the coast (Fig. 1(a), $r^2 = 0.95$ using a linear regression of total surface ^{234}Th vs. distance). Particulate ^{234}Th ($>1\ \mu$m) ranged between 20 and 50% of the total measured activity (Table 1). In contrast, total ^{7}Be activities showed no clear gradient between onshore and offshore waters, and with the exception of one station, ranged from 91 to 381 d.p.m. m^{-3} (Fig. 2(a), $r^2 < 0.1$). Particulate ^{7}Be concentrations never exceeded 11% of the total measured activity.

In April, just prior to our cruise, a large storm struck Wilkinson Basin. Whereas previous studies have shown the spring bloom to be fully underway by the beginning to middle of April (Bigelow, 1926a,b; Gran and Braaurd, 1935; Townsend and
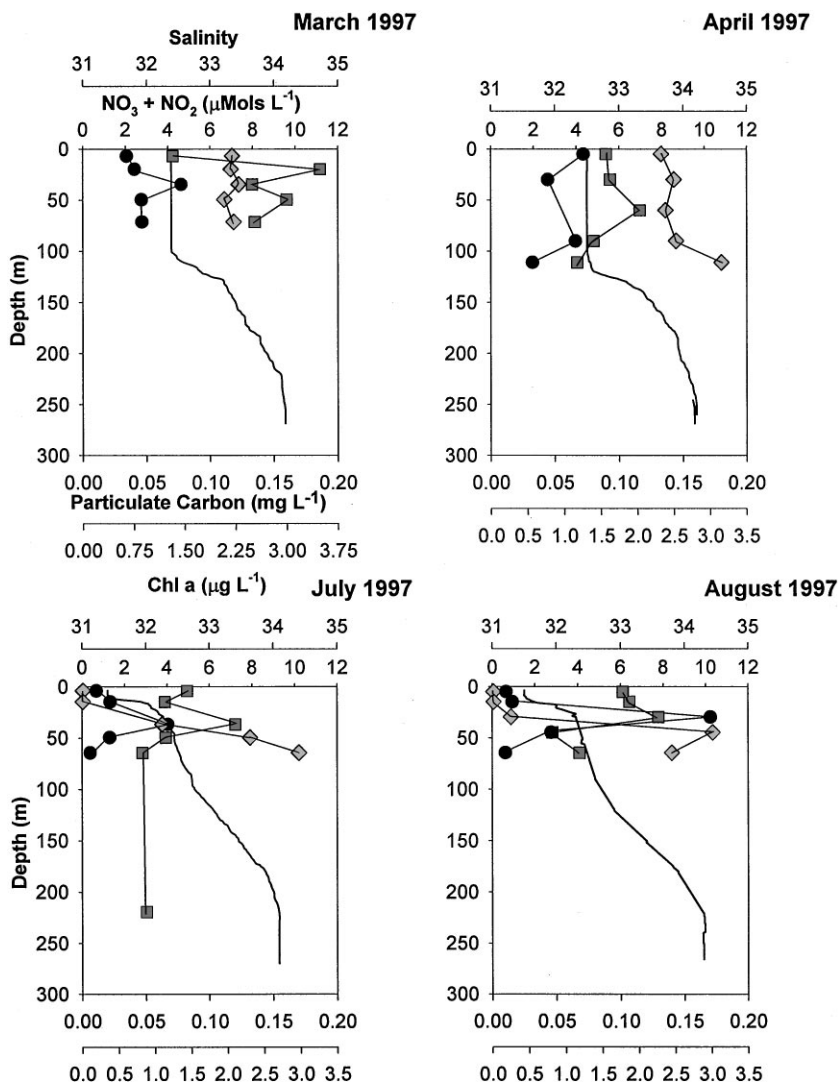
Fig. 3. Depth profiles of salinity (black line), $NO_3 + NO_2$ (diamonds), particulate organic carbon (squares) and chl a (circles). Note the decrease in mixed layer depth from March to August and the formation of a large subsurface chl a maximum.

Spinrad, 1986; Durbin et al., 1995), there was little evidence that this was occurring within Wilkinson Basin in April 1997. This was probably due to a lack of shallow stratification, as mixed layer depths actually increased from 100–110 m after the storm, rather than decreasing to approximately 40–60 m as observed in previous studies of this region (Townsend and Spinrad, 1986; Durbin et al., 1995). Surface activities of ^{234}Th were on average higher than in March (1.21 $\pm$ 0.26 vs. 0.96 $\pm$ 0.20)

and ranged from 0.6 to 1.8 d.p.m. L^{-1}, with a single offshore elevated value of 2.2 d.p.m. L^{-1} (Fig. 1(b)). Total ^{234}Th again increased with greater distance from shore ($r^2 = 0.57$, excluding st. 13). Particulate ^{234}Th activities were still high and similar in range to those measured in March. Total ^{7}Be concentrations were significantly higher than in March, ranging from 180 to 512 d.p.m. m^{-3}. However, there was still no clear gradient in concentration with increasing distance from the coast (Fig. 2(b), $r^2 < 0.1$). Higher ^{7}Be activities were the result of the substantial increase in ^{7}Be input due to rainfall that occurred during the large storm that struck the southwestern Gulf of Maine between the March and April cruises (Benitez-Nelson and Buesseler, 1999a). Particulate ^{7}Be concentrations were still less than 10% of the total ^{7}Be measured activity.

In the early summer increasing thermal stratification and nutrient uptake following the spring bloom resulted in low nutrient waters, which persisted through the August cruise. In July, total surface water ^{234}Th activities ranged from 0.5 to 1.65 d.p.m. L^{-1}, with particulate concentrations between 20 and 50% of the total (Fig. 1(c)). Although there was a significant offshore gradient in total ^{234}Th activity, the magnitude of this gradient was less than that found in April ($r^2 = 0.41$). ^{7}Be activities ranged from 198 to 600 d.p.m. m^{-3} and again showed no clear offshore gradient (Fig. 2(c), $r^2 < 0.1$). Particulate ^{7}Be concentrations were less than 10% of the total measured ^{7}Be activity. In August, total surface water ^{234}Th activities and their spatial distribution were similar in range to those found in July (Fig. 1(d), $r^2 = 0.41$). Particulate ^{234}Th activities decreased to values that were typically less than 20% of the total measured ^{234}Th activity. ^{7}Be concentrations and offshore distribution were similar to those found in July (Fig. 2(d)). Particulate ^{7}Be concentrations, however, decreased to less than 5% of the total measured ^{7}Be activity.

Depth profiles of ^{234}Th and ^{7}Be activities at station 7 in Wilkinson Basin are given in Table 1 and Figs. 4 and 5. In March and April, both dissolved and particulate ^{234}Th and ^{7}Be concentrations remained relatively constant with depth. Although in April, both total ^{234}Th and ^{7}Be activities increased by close to factor of 1.5 over the upper 75 m. In July, total ^{234}Th activities increased with depth below the 8 m mixed layer, reaching equilibrium values at 65 m. In contrast, total ^{7}Be activities decreased by a factor of two between the mixed layer and deeper waters. In August, ^{234}Th activities actually decreased to a minimum at 30 m, the depth of the Chl *a* maximum, and remained low to 55 m. ^{7}Be activities, on the other hand, were high only in the upper 30 m, decreasing rapidly to near zero at depth. Increased errors on ^{7}Be activities in August were due to the longer time period between sample collection and measurement.

4. Discussion

4.1. ^{234}Th derived particle export

^{234}Th is a naturally occurring particle-reactive radionuclide which has been commonly used to study particle scavenging and organic carbon export in the upper ocean (Santchi et al., 1979; Kaufman et al., 1981; Coale and Bruland, 1985, 1987;
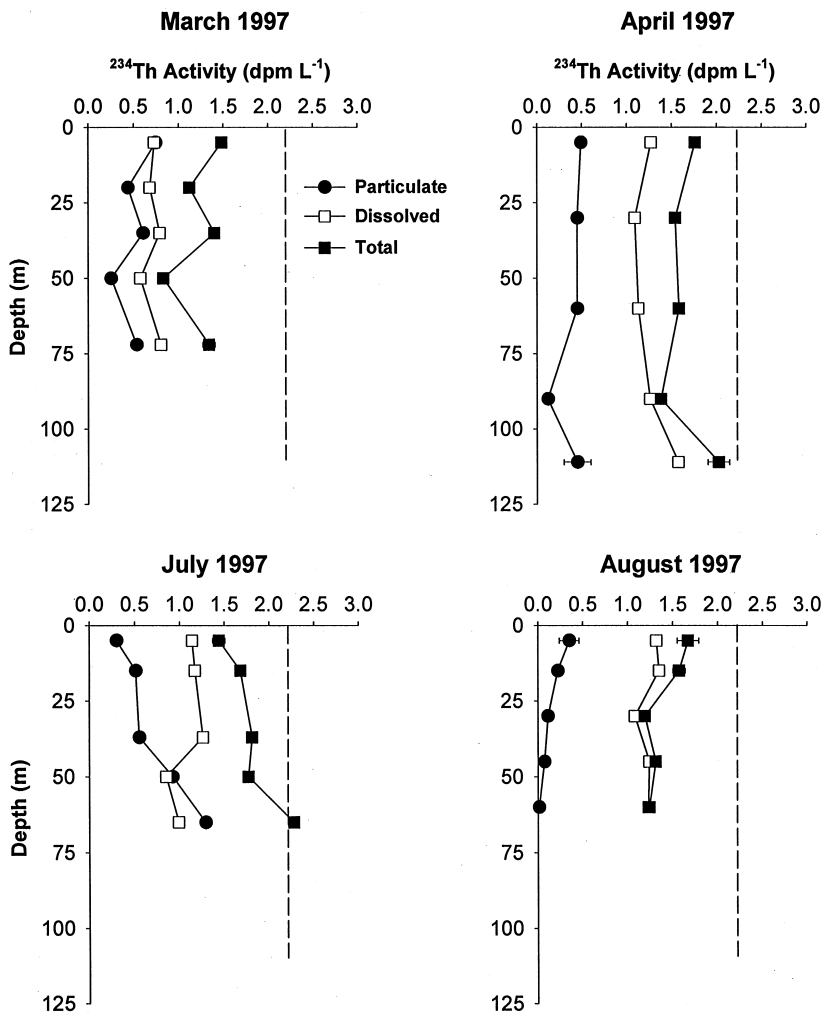
Fig. 4. Particulate (closed circles), dissolved (open squares), and total ^{234}Th (closed squares) activities in d.p.m. L^{-1} with depth. Dashed lines are representative of ^{238}U activities. Error bars are 1σ.

Murray et al., 1989; Buesseler et al., 1992, 1994, 1998; Bacon et al., 1996; Murray et al., 1996). Since the half-life of ^{234}Th is 24.1 d, the disequilibrium between its non-reactive conservative parent ^{238}U and the measured ^{234}Th activity reflects the net rate of particle export from the upper ocean on time scales of days to weeks. In the open ocean, the observed ^{234}Th distribution is controlled by the rates of formation of fresh particle surfaces due to biological processes and the formation of sinking particles due to grazing and aggregation. In coastal environments, however, surface ^{234}Th activities will also reflect enhanced removal due to mixing and resuspension of sediments, i.e. non-biological processes.
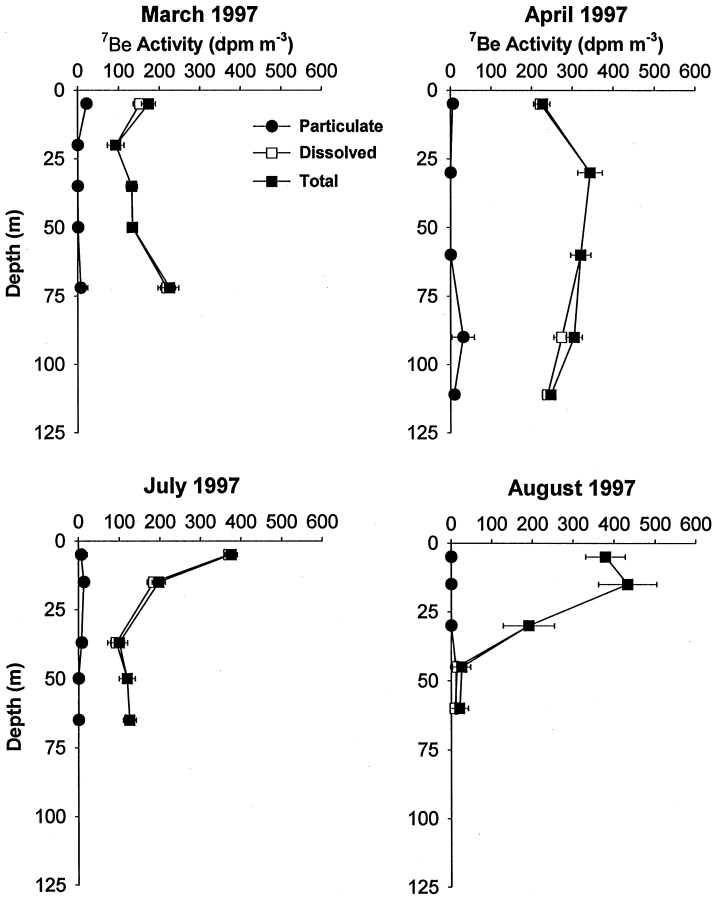
Fig. 5. Particulate (closed circles), dissolved (open squares), and total ^{7}Be (closed squares) activities in d.p.m. m^{-3} with depth. Error bars are 1σ.

In this study, surface ^{234}Th activities were measured at stations of substantially diverse and shallow bottom topography (40–280 m). As a result, disequilibrium between ^{234}Th and ^{238}U is most likely caused by a combination of both boundary scavenging and biologically driven export. The first process might be expected to dominate in the winter when biological production is low and storm activity causes more intense vertical mixing. In contrast, biologically enhanced removal would become more important in the spring and summer with increasing production and grazing.

In order to determine the flux of particulate matter from the upper ocean, the following ^{234}Th activity balance equation is used:

$$\mathrm{d}A_{\mathrm{Th}}/\mathrm{d}t = A_{\mathrm{U}}\lambda - A_{\mathrm{Th}}\lambda - P + V \tag{1}$$

where dA_{Th}/dt is the change in ^{234}Th activity with time, A_U is the ^{238}U activity (^{238}U (d.p.m. L^{-1}) = 0.0686 Salinity; Chen et al., 1986), A_{Th} is the total measured ^{234}Th activity, λ is the decay constant for ^{234}Th (= 0.0288 d^{-1}), P is the net removal flux of ^{234}Th on particles, and V is the sum of advective and diffusive terms. In the open ocean, the magnitude of the export flux is most often driven by the extent of the ^{234}Th/^{238}U disequilibrium. Steady state (SS) is often assumed ($dA_{Th}/dt = 0$) and physical processes ignored.

The use of NSS ^{234}Th formulations appears to be important during plankton blooms, when significant ^{234}Th removal can occur (Buesseler et al., 1992a, 1998; Cochran et al., 1995, 1997). More commonly, however, SS models are sufficient (Tanaka et al., 1983; Moran and Buesseler, 1993). Vertical advection, V in Eq. (1), has been shown to be significant in areas of intense upwelling, such as in the Equatorial Pacific and along the coast of the Arabian Sea during the SW Monsoon (Buesseler et al., 1995, 1998; Bacon et al., 1996). In addition, horizontal ^{234}Th transport can be important in coastal regions, especially in bays, where large horizontal gradients in ^{234}Th scavenging can occur (McKee et al., 1984; Wei and Murray, 1992; Gustafsson et al., 1998).

The general circulation of the Gulf of Maine is complex and driven by a combination of processes such as wind stress, strong tidal forcing, and spring riverine discharge (Brooks, 1991). Water mass circulation in the Gulf is cyclonic and controlled to a large extent by uneven bottom topography. The majority of the Maine Coastal Current flows southward from Penobscot Bay, along the shoreline, and through the Great South Channel. Current intensification in the spring results from interactions between springtime river runoff from the Scotian Shelf and high salinity waters from the Atlantic (Brooks, 1985). Because of the seasonality expected in physical transport and biological processes and the near-shore nature of our sampling sites, we have sought to understand the relative effects of NSS and physical processes, such as horizontal advection, on the measured ^{234}Th budgets.

As stated previously, our sampling sites covered a large range of shallow and deep sites. Mixed layer depths (defined by a change in density ≥ 0.125 kg m^{-3}) varied not only seasonally, but spatially as well. At some inshore stations, mixing often occurred down to the sediment/water interface. In order to compare the temporal and spatial variability of surface export we used our surface data to calculate sinking fluxes at a depth of 10 m. As a result, at most stations this is a minimum flux. We cannot extrapolate below this depth without complete profiles of ^{234}Th, since there is significant chemical heterogeneity within the mixed layer (as evidenced by our st. 7 depth profiles, Figs. 3 and 4; Benitez-Nelson and Buesseler, 1999b). At station 7 we can extend our analyses down to 50 m.

4.2. ^{234}Th Flux Model

In order to fully understand the effects of SS, NSS, and physical processes in deriving ^{234}Th export, we have broken down Eq. (1) into several mathematical terms, where $(A_U - A_{Th})\lambda$ is defined as the SS term, dA_{Th}/dt is defined as the NSS term, and V takes into account physical processes. Our surface ^{234}Th data was first placed onto
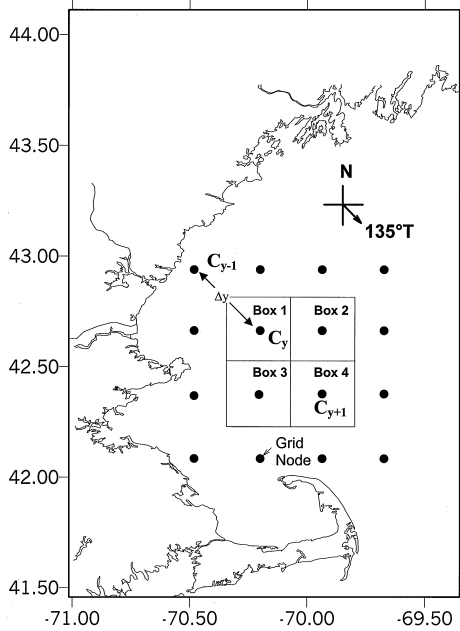
Fig. 6. Schematic of multi-dimensional non-steady state box model. Circles depict grid nodes. Boxes are numbered clockwise stating at the northwestern most box. Both advective and diffusive flow is to the south at 135° of true North.

a regularly spaced 16 point grid using a linear kriging technique (Fig. 6; SURFER™). In March, there were too few offshore data points to obtain a full grid. In the center of the grid, we have defined 4 boxes, 2 inshore (#1 and #3) and two offshore boxes (#2 and #4) in which we compare the magnitude of each of the terms defined above.

If SS is assumed, the difference in the total ^{234}Th activity from equilibrium values drives the magnitude of the ^{234}Th particulate export flux, such that the greater the deficit, the larger the particulate export. The NSS term, dA_{Th}/dt in Eq. (1), takes into account any temporal changes in ^{234}Th activities, a circumstance that can occur during and after phytoplankton blooms. In general, decreasing ^{234}Th inventories with time will result in a calculated SS particulate export that is too low, since the true flux must be larger to result in the observed decrease in ^{234}Th. In contrast, if ^{234}Th activities increase with time, the SS particulate export estimates would be erroneously high.

The change in activity with time, dA_{Th}/dt (Eq. (1)), was determined for April, using March data, and for August using data taken in July $(A_2^t - A_1^t)/\Delta t)$. This determination assumes that the activity change took place within a single water mass. We maintain that this is appropriate for the month long interval separating our spring and summer cruises, given the ^{234}Th mean life of 35 days. However, we do not use this assumption for the longer 3 month time period between the April and July cruises. In

April, [234]Th activities used in the NSS calculation were interpolated from stations closest in proximity to the box of interest from the proceeding March cruise.

Physical processes such as horizontal advection and diffusion are often ignored in calculating [234]Th particulate export due to the difficulty associated with estimating the magnitude of horizontal transport fluxes. In addition, calculations require good spatial coverage of the [234]Th activity distribution within a study site. In many cases, time and budget constraints do not allow for such measurements to be made. However, recent investigations in coastal environments demonstrate that these processes cannot be disregarded in [234]Th flux estimates (Gustafsson et al., 1998).

The physical process term, V in Eq. (1), can be rewritten as

$$V = - u \mathrm{d}A_{\mathrm{Th}}/\mathrm{d}x - v \mathrm{d}A_{\mathrm{Th}}/\mathrm{d}y + K_x \mathrm{d}^2 A_{\mathrm{Th}}/\mathrm{d}x^2 + K_y \mathrm{d}^2 A_{\mathrm{Th}}/\mathrm{d}y^2 \tag{2}$$

where u and v are the velocities in the chosen x and y direction, respectively, $\mathrm{d}A_{\mathrm{Th}}/\mathrm{d}x$ is the activity gradient along the x-axis, $\mathrm{d}A_{\mathrm{Th}}/\mathrm{d}y$ is the activity gradient along the chosen y axis, K_x and K_y are the x and y horizontal diffusivities, respectively, and $\mathrm{d}^2 A_{\mathrm{Th}}/\mathrm{d}x^2$ and $\mathrm{d}^2 A_{\mathrm{Th}}/\mathrm{d}y^2$, the second derivative of the activity distribution. Note that this formulation does not consider upwelling of higher activity [234]Th from deep waters due to the lack of regional depth profiles in this study (see below).

Horizontal advection directions and rates were not measured during our cruises. Therefore, historical measurements derived from surface current meter measurements in close proximity to our stations were used in conjunction with drifter simulations using a Gulf of Maine circulation model described by Naimie (1996). Two sets of current meter data were used. The first set consists of data taken during November 1974 to December 1975 at a depth of 33 m (Vermersch et al., 1978). The second set consists of data taken from June to August of 1983 and 1984 at a depth of 25 m (Brooks, 1985; Gottlieb and Brooks, 1986). Both data sets show that the dominant water flow at our study site is along the coast to the South or Southwest. Drifter track model simulations and actual drifter track measurements made in the spring of 1993 and 1994 further support this alongshore direction (R. Geyer, personal communication; Naimie, 1996).

The day to day intensity of the alongshore and offshore current is highly variable. However, 1–3 month long integrated current measurements taken from different years are similar, and indicate an average alongshore current velocity of 5–13 cm s^{-1} and an average offshore current velocity of -2 to 4 cm s^{-1} (Vermersch et al., 1985; Gottlieb and Brooks, 1986; R. Geyer, pers. comm.). The activity distribution of [234]Th at any particular point in time reflects the net [234]Th source and/or sink over the mean life ($1/\lambda \approx 35$ d) of [234]Th. Thus, while horizontal advective velocities may vary significantly over day to several week long time scales, it is necessary to use the *average* current velocity integrated over longer, month long time periods. In this study, a current velocity of 1 cm s^{-1} moving directly offshore was used ($\sim 135°$ from true North). A coordinate system was set such that $v \, \mathrm{d}A_{\mathrm{Th}}/\mathrm{d}y$ in Eq. (2) was zero.

Surface [234]Th distributions show north/south patterns which, for the most part follow the coastline along the dominant direction of water flow during each cruise (based on drogue simulations; Naimie, 1996). Thus, alongshore gradients in the [234]Th activity tended to be small, resulting in low net [234]Th transport parallel to the coast.

In contrast, significantly larger gradients in ^{234}Th activity occurred with increasing distance from shore. Similar ^{234}Th distributions both alongshore and offshore have been found in the Arabian Sea and Casco Bay in the Gulf of Maine (Buesseler et al., 1998; Gustafsson et al., 1998).

Horizontal diffusion estimates were obtained using Okubo's (1971) empirically derived oceanic diffusion diagrams. Confidence in these estimates arises from the fact that our study site is similar in nature to those (i.e. New York Bight) used to develop Okubo's empirically derived diffusion estimates. The distance, or 'length scale' between each station ranged from 10 to 40 km. This yielded an apparent diffusivity of $0.8 \times 10^5 – 4.0 \times 10^5$ cm^2 s^{-1}. These estimates are significantly lower than those used by Gustafsson et al. (1998) in nearby Casco Bay. The Casco Bay study differs from ours as it was conducted at sites closer inshore and within a tidal strait, where tidally induced high shear rates occur (Gustafsson et al., 1998). Gustafsson et al. (1998) found that horizontal advective transport within inner and outer Casco Bay was insignificant relative to dispersion and particulate export. In addition, dispersive properties were substantial within inner Casco Bay only during one of the two cruises.

Using our box model, we simplified Eq. (2) into the following box model equation (Fig. 6):

$$V = v(C_{y+1} - C_{y-1})/(2\Delta y) + K_y(C_{y-1} - 2C_y + C_{y+1})/\Delta y^2 \qquad (3)$$

where Δy is the distance between grid nodes, C_y is the ^{234}Th concentration within the box, and C_{y+1} and C_{y-1} are the ^{234}Th activities on either side of each box. Distances between grid nodes were 33.2 km. This was equivalent to an Okubo (1971) derived apparent diffusivity of $K_y = 3.2 \times 10^5$ cm^2 s^{-1}.

4.3. ^{234}Th flux model results

Results from our modeling efforts are shown in Fig. 7. In this figure, we compare the magnitude of each term from Eq. (1). Note that Eq. (1) has the particulate export flux, P, as positive for fluxes from the surface to depth. The SS term, $(A_U\lambda - A_{Th}\lambda)$ represents the difference between the ^{234}Th activity expected from ^{238}U decay and that actually measured. The NSS term (dA_{Th}/dt) takes into account that ^{234}Th activities may change with time. If (dA_{Th}/dt) is negative, this implies that the ^{234}Th inventory has decreased from one sampling period to another. Therefore, there must be more export occurring than what would have been found had SS been assumed. Thus, the NSS term is assigned a positive value, since there is an increase in the flux from the surface to depth. In April, July, and August the advection/diffusion term (V in Eq. (3)) reflects the transport of low ^{234}Th activity waters to areas of higher activity. This low ^{234}Th activity results in the 'appearance' of more particulate export than what has actually occurred. As a result, the advection/diffusion term must be negative, since there is a decrease in the flux from surface to depth.

The uncertainty associated with gridding was determined by taking the difference between the ^{234}Th activity measured at a specific station with the ^{234}Th activity interpolated from the gridded data at that station. Overall errors are determined from the average uncertainties associated with gridding, ^{234}Th collection efficiencies, and
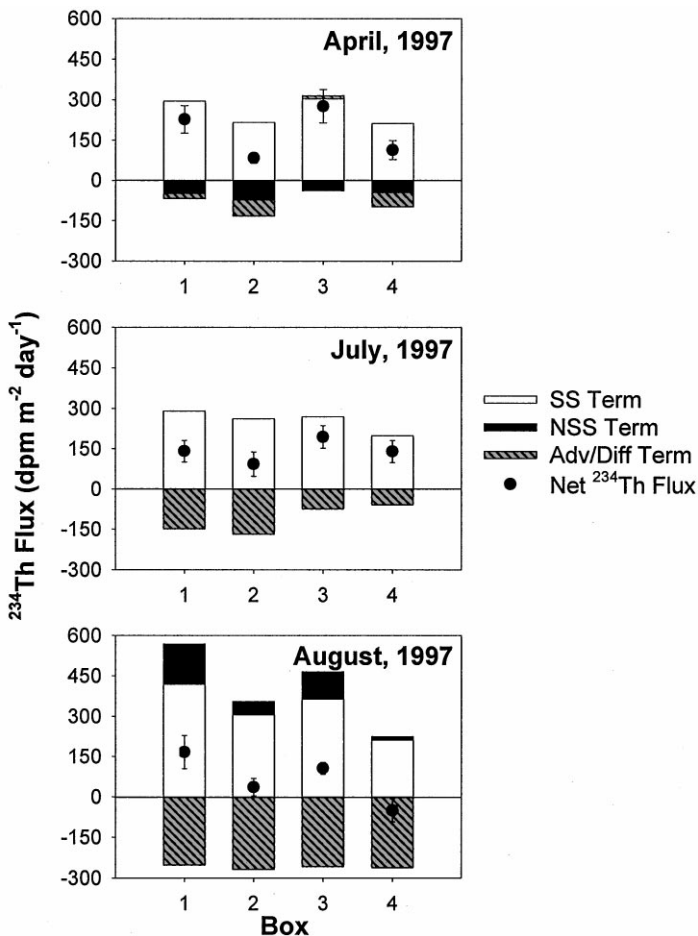
Fig. 7. ^{234}Th model flux results for the April, July and August cruises. Each stacked bar represents the magnitude of the steady-state term ($A_U\lambda - A_{Th}\lambda$; white), non-steady state term (dA_{Th}/dt; black) and advection/diffusion term (V; light gray). All fluxes were integrated over the upper 10 m and are in d.p.m. m^{-2} d^{-1}. The net ^{234}Th flux (black circles) from the inclusion of all three terms is also shown.

counting statistics. Possible errors derived from current velocities and diffusion coefficients were not included.

From Fig. 7 it is clear that two major components driving the surface ocean export flux of ^{234}Th are the SS and physical process terms. The incorporation of both advection and diffusion terms reduced the net ^{234}Th export flux. In August, when ^{234}Th gradients were largest, ^{234}Th fluxes decreased by $>100\%$ due to NSS and physical processes (Table 2). ^{234}Th derived particulate export fluxes were always greater in the nearshore boxes (e.g. 1 and 3) than in the offshore boxes (e.g. 2 and 4).

Table 2
Steady state (SS), non-steady state (NSS), and advection/diffusion model results. ^{234}Th derived POC export rates were determined over the upper 10 m only

Box	SS ^{234}Th export at 10 m (d.p.m. m^{-2} d^{-1})	SS POC export at 10 m (mmol m^{-2} d^{-1})	NSS ^{234}Th export at 10 m (d.p.m. m^{-2} d^{-1})	NSS POC export at 10 m (mmol m^{-2} d^{-1})	NSS + Adv./Diff. ^{234}Th export at 10 m (d.p.m. m^{-2} d^{-1})	NSS + Adv./Diff. POC export at 10 m (mmol m^{-2} d^{-1})
April 1	295 ± 33	7.7 ± 1.2	246 ± 39	6.4 ± 1.3	227 ± 51	4.9 ± 1.6
2	216 ± 29	4.4 ± 0.9	143 ± 23	2.9 ± 0.6	83 ± 19	1.7 ± 0.6
3	303 ± 32	9.4 ± 1.6	264 ± 44	8.2 ± 1.7	276 ± 62	10.1 ± 2.7
4	212 ± 30	7.0 ± 1.3	167 ± 37	5.5 ± 1.4	113 ± 35	3.3 ± 1.2
July 1	290 ± 28	11 ± 2	—	—	144 ± 40	3.4 ± 1.4
2	262 ± 32	7.1 ± 1.8	—	—	73 ± 45	1.7 ± 1.1
3	269 ± 30	8.3 ± 1.6	—	—	209 ± 42	5.7 ± 1.9
4	199 ± 29	5.7 ± 1.5	—	—	146 ± 41	4.6 ± 1.6
August 1	419 ± 48	48 ± 16	568 ± 75	66 ± 22	166 ± 62	19.1 ± 7.0
2	305 ± 40	18 ± 7	355 ± 33	21 ± 7	36 ± 32	1.8 ± 1.1
3	364 ± 26	35 ± 12	475 ± 32	46 ± 16	106 ± 22	8.1 ± 10.0
4	211 ± 24	3.2 ± 1.3	224 ± 67	3.4 ± 1.7	− 51 ± 42	—

In August, a net negative ^{234}Th flux was determined for the southeastern most box ($\#4$). Two processes can cause negative ^{234}Th particulate export fluxes. Either there was upwelling of high ^{234}Th concentrations from depth, i.e. from sub-surface re-mineralization, or the terms describing the ^{234}Th budget at that box were not properly constrained. The above calculation is highly dependent on the chosen current velocities, horizontal diffusion coefficients and measured ^{234}Th activity gradients (e.g. Eq. (3)). The largest uncertainty is almost certainly associated with the chosen historical current velocities. Doubling the advective offshore current velocity, v, results in a decrease in the ^{234}Th export flux by greater than 50% in April and July, and greater than 250% in August. In contrast, doubling the horizontal eddy diffusivity, K_y, increases the ^{234}Th export flux by less than 30%. Increasing or decreasing the first and second order activity gradients (e.g. dA_{Th}/dx and $d2A_{Th}/dx^2$ in Eq. (2)) results in similar magnitude changes in the ^{234}Th export for the April, July, and August cruises. However, based on differences between measured and gridded ^{234}Th activities, and errors on the measured ^{234}Th activities, average combined uncertainties in the first and second order activity gradients are 30%. This uncertainty is smaller than that expected from using advective fluxes based upon the historical current velocity values.

An underestimation of particulate export rates will occur if deep waters with higher ^{234}Th activity are substantially transported into low activity surface waters. It is difficult to predict the extent of this effect on the 10 m integrated ^{234}Th flux with only surface measurements of ^{234}Th. Nonetheless, one can gauge the importance of this process by using the depth distribution of ^{234}Th at station 7 and the vertical eddy diffusivity rates found from ^{7}Be during the July and August cruises (see *Vertical Eddy Diffusivity* (K_z)). In July, the vertical eddy diffusivity flux of ^{234}Th into the upper 10 m derived from ^{7}Be was determined to be 26 d.p.m. m^{-2} d^{-1}. This would result in less than a 10% increase in the SS ^{234}Th export flux of 206 ± 36 d.p.m. m^{-2} d^{-1} and is well within the error of the calculated SS flux. In August, deep waters are actually lower in ^{234}Th activity than that observed at the surface. As a result, the upper 10 m NSS ^{234}Th export flux is actually reduced from 144 ± 13 to 130 d.p.m. m^{-2} d^{-1} (10%).

Our simple box model demonstrates the complexity involved in trying to evaluate the effect of physical processes, such as horizontal advection, in a coastal marine environment, especially when there are large gradients in ^{234}Th activity over small spatial scales. These physical processes do not pertain to ^{234}Th alone and would be true for any mass balance of N, P, or even O_2 within a coastal system. Many open ocean regimes also have significant regional variability in ^{234}Th activity, but this often occurs over much larger spatial scales, such that dA/dx and dA/dy (from Eq. (2)) are relatively small (Buesseler et al., 1995, 1998). In addition, total ^{234}Th activities are often integrated over depth intervals, which are much larger than those used in the above calculations (100 versus 10 m). This requires the use of depth integrated horizontal current velocities which are substantially smaller than those at the surface. As a result, the V term in Eq. (1) is substantially reduced in the open ocean as opposed to coastal environments. Our study in Wilkinson Basin indicates that understanding the magnitude and direction of coastal currents is a major issue for accurately

determining ^{234}Th particulate export fluxes in coastal waters. Future work in coastal regimes must consider these processes.

4.4. Particulate organic carbon/^{234}Th ratios

The export fluxes of particulate organic C can be calculated as the product of the predicted ^{234}Th flux and the site and time specific measurements of particulate organic C (POC) to particulate ^{234}Th (Buesseler et al., 1992a). The POC/^{234}Th ratio has been found to vary seasonally, spatially, and generally decreases with increasing water depth (Buesseler et al., 1992a, 1998; Moran et al., 1993; Buesseler, 1998). This ratio has also been found to vary depending upon whether filters of small or large pore diameters were employed, or if sediment traps were used for the determination of POC/^{234}Th ratios (Buesseler et al., 1992a, 1995, 1998; Moran et al., 1993; Murray et al., 1996). Thus, while some uncertainty remains in the absolute value of the POC/^{234}Th derived fluxes, the relative values within any one study using any single sampling technique should remain robust. Even if biological particles do not dominate the sinking phases, any particulate phases that are not biologically derived should be reflected in the bulk POC/^{234}Th ratio. For example, the presence of aluminosilicates would tend to lower the measured POC/^{234}Th ratio and, thus the calculated POC export flux. As long as the ratio is representative of the bulk material responsible for export, this empirical approach should hold for a given site and time.

In this study, we used a combination of bottle POC data (2–4 L filtered onto GF/F filters) and large volume particulate ^{234}Th samples (200–400 L filtered onto 1 μm cartridge filters) for the determination of POC/^{234}Th on particles. Similar sample sizes and filters were used in the North Atlantic Bloom Experiment by Buesseler et al. (1992a). Surface POC concentrations ranged from an average low of 7.5 μM POC in March to an average high of 14 μm POC in April. Within the upper 10 m, the ratio of POC/^{234}Th varied dramatically: from 5 to 8 μmol/d.p.m. in March to 9 to 113 μmol/d.p.m. in August (Table 1). Values greater than 113 μmol/d.p.m. in August have large associated errors ($\pm 100\%$) due to very low particulate ^{234}Th. Seasonal and spatial differences in POC/^{234}Th ratios were therefore almost entirely due to changes in the measured particulate ^{234}Th distribution.

Several studies have found significant differences in the POC/^{234}Th as a result of sampling technique. Murray et al. (1996) found that POC/^{234}Th ratios in 1 μm particles collected from Nisken bottles were 2–4 times higher than ratios measured on small particles collected by in situ pumps. Moran et al. (2000), have recently suggested that bottle derived POC data may overestimate true POC levels, due in part to adsorption of DOC onto the filter and hence a high filter blank on small volume samples. These researchers found POC concentrations to be 2–4 times higher in small volume (~ 1–2 L) versus large volume (~ 100–600 L) samples. This artifact in the small volume bottle POC data could explain the differences in POC/^{234}Th between bottle and in situ pump data originally noted by Murray et al. (1996). Coastal areas might be expected to exhibit smaller DOC adsorption affects given their high POC concentrations.

The ratio of POC/^{234}Th has also been found to be significantly different between sediment trap samples and those collected using large volume in situ pumps (Buesseler et al., 1992a; Murray et al., 1996). In the Equatorial Pacific, sediment trap POC/^{234}Th ratios were 3 times higher than those collected using in situ pumps (Murray et al., 1996). In the North Atlantic, however, trap POC/^{234}Th ratios were 2–4 times lower (Buesseler et al., 1992). The reasons for these differences between the two sampling techniques are unclear, but may be related to possible 'swimmer' contamination within trap samples, or to the fact that in situ pumps may not accurately collect sinking material. This issue is currently unresolved.

Confidence in our POC/^{234}Th data is gained by comparing our small sample volume (2 L) depth profiles of POC/^{234}Th found at Wilkinson Basin (st. 7) to those measured using large volume (100–1500 L) in situ pumps (Charette et al., 2000). POC concentrations were typically lowest at the Wilkinson Basin site. Thus, the effects of any DOC adsorption that would potentially elevate our POC numbers are expected to be maximized there. Charette et al. (2000) measured depth profiles of the ratio of POC/^{234}Th in Wilkinson Basin in March, June and September 1995. Their average POC/^{234}Th ratio measured over the upper 50 m was 12.8 ± 1.9 μmol/ d.p.m. and is, within error, the same as the average POC/^{234}Th ratio of 14.4 ± 4.3 μmol/d.p.m. measured in this study. Our larger standard deviation is almost entirely due to the particulate ^{234}Th activity measured in August 1997, which is on average, 20% lower than that measured by Charette et al. (2000) in September 1995.

The depth dependence of POC/^{234}Th ratios indicate that ^{234}Th derived POC export can be very sensitive to the chosen depth of integration. However, in this study obvious gradients in POC/^{234}Th ratios with depth only occurred in July (Table 1). As a result, an average POC/^{234}Th ratio over the upper 50 m was used to determine POC fluxes for each cruise. Only POC/^{234}Th ratios with errors less than 50% were used to calculate POC/^{234}Th ratios in August.

4.5. Particulate organic carbon export fluxes

Surface POC export fluxes were determined for each of the four boxes (Figs. 6 and 7) using the NSS physical model (physical model only in July) described above and gridded POC/^{234}Th data from each cruise (Table 2). Errors are determined from the propagation of uncertainties associated with gridding (similar to ^{234}Th, see above) and measurement of POC concentrations and ^{234}Th activities. Not surprisingly, POC export was higher within the inshore boxes (#1 and #3) than in the offshore boxes (#2 and #4) during the April, July and August cruises. However, differences were most apparent in April and in August. In August, inshore POC export was almost an order of magnitude greater, while in April, POC export was only three times higher than in the offshore boxes. Average POC export over all boxes and cruises was 6.2 ± 2.6 mmol C m^{-2} d^{-1}.

At station 7, depth profiles of ^{234}Th enabled SS (March and July) and NSS (April and August) estimates of particulate carbon export over the average depth of the

Table 3
Depth-integrated SS and NSS model results. Particulate organic carbon export rates from the upper 50 m were obtained for the April and August cruises by multiplying the NSS ^{234}Th particulate flux by the ratio of POC/^{234}Th at ~ 50 m (from Table 1, see text). In March and July, particulate organic carbon fluxes were determined using the SS model only. Error bars are 1σ (see text)

Cruise	SS particulate export at 50 m (d.p.m. m^{-2} d^{-1})	NSS particulate export at 50 m (d.p.m. m^{-2} d^{-1})	POC export at 50 m (mmol m^{-2} d^{-1})
March, Station 7	1460 ± 180	—	15 ± 8
April, Station 7	821 ± 74	18 ± 3	0.3 ± 0.1
July, Station 7	574 ± 51	—	7 ± 3
August, Station 7	1141 ± 109	1689 ± 239	36 ± 20

euphotic zone (0.1% surface irradiance ranged from 35 m (August) to 85 m (March), average: ~ 50 m; Table 3). Increasing the depth interval from 10 to 50 m enables the inclusion of subsurface production, such as indicated by subsurface chl *a* maximums, which generally results in an increase in ^{234}Th scavenging. Integrating to depths greater than 50 m, however, may also result in the inclusion of resuspended sediments, which are brought into the upper water column by trawling activity (Pilskaln and Lehmann, 1998). We were not interested in including these bottom scavenging processes in our analyses of the overall seasonal export patterns.

POC fluxes were high in March at the onset of the spring bloom (Table 3). Similar high POC fluxes have been seen during the North Atlantic Bloom Experiment and at high latitudes, such as in the Arctic (Cochran et al., 1995, 1997). A secondary maxima in particulate organic carbon export occurred in August. Speciation analyses of plankton tows collected in August indicated that the water column was dominated by a large assemblage of copepods in various stages of their life cycle. Abundances were substantially larger than those found during the July cruise. Thus, the increased particulate export in August was most likely the result of increased zooplankton grazing and fecal pellet production within the euphotic zone. The average particulate organic carbon NSS (SS for March) export rate averaged over the upper 50 m at station 7 was 14.4 ± 13.5 mmol C m^{-2} d^{-1}, almost an order of magnitude greater than that found at this station for the upper 10 m alone.

Although the effects of horizontal advective and diffusive mixing were not determined for our depth profile station (st. 7), it is expected that these processes are significantly smaller in magnitude than that determined for the upper 10 m. While offshore gradients in depth integrated ^{234}Th export fluxes may be similar in magnitude, depth integrated horizontal current velocities are significantly lower than that at the surface. Current meter readings taken at various depths close to our study site also show an exponential decrease in offshore current speed with increasing water depth (to 50 m; W.R. Geyer, pers. comm.). Similar results have been found in the Arabian Sea and in the Equatorial Pacific (Buesseler et al., 1995, 1998).

Our depth integrated results are similar to the [234]Th derived POC export rates of 20 mmol C m^{-2} d^{-1} estimated using the same approach for 50 m in the central Gulf of Maine in March, June, and September 1995 (Charette et al., 2000). Some differences are to be expected due to interannual variability within Wilkinson Basin. Also it should be noted that Charette et al. (2000) used a SS model and the POC/[234]Th ratio found on 53 μm pore diameter filters to derive their POC fluxes. Their POC/[234]Th ratio was, on average, greater than 2 times that used in this study. Hence the similarity in fluxes may be fortuitous.

The ratio of [234]Th derived POC export to primary production was defined as the *ThE* ratio by Buesseler (1998). While primary production was not measured in this study, it is still useful to compare our [234]Th derived POC export to historical measurements of primary productivity in order to place our results in context of other [234]Th derived POC export studies. There are few primary production rate estimates within the Gulf of Maine. O'Reilly and Busch (1984) estimated a Gulf wide annual primary production rate of 24.2 mol C m^{-2} yr^{-1} (66.2 mmol C m^{-2} d^{-1}) over the depth of the euphotic zone from 21 surveys which took place from 1978 to 1980. Charette et al. (2000), measured euphotic zone integrated primary production rates of 29.6 mmol C m^{-2} d^{-1} at a station close in proximity to our Wilkinson Basin site in August and September 1997. The O'Reilly and Busch (1984) study, although conducted before the advent of 'clean' techniques (Fitzwater et al., 1982), is most likely a maximum estimate of primary production at our site, since it includes the much higher primary productivity waters located in the northeastern Gulf of Maine (e.g. Jordan Basin). In contrast, the Charette et al. (2000) estimate may be considered a minimum, since their estimates did not include the high primary production estimates typically found during the spring bloom.

Using the primary production estimates from above, surface ocean *ThE* ratios ranged from 9 to 21%. Depth integrated (50 m) *ThE* ratios ranged from 22 to 49%. These results are similar to the August and September 1997 depth integrated *ThE* ratios of 26% calculated by Charette et al. (1996, 2000) for the entire gulf of Maine. The *ThE* ratio found in the Gulf of Maine is similar to that found in other productive regimes, such as in high latitudes, the Arabian Sea during the late SW Monsoon, and the North Atlantic Bloom Experiment (e.g. Buesseler, 1998). Care must be taken to note the depth of integration when comparing *ThE* ratios from other regimes as increasing the depth of integration can generally result in higher export ratios, until a depth is reached where remineralzation rates are greater than the increase in particle fluxes.

4.6. Vertical eddy diffusivity (K_z)

Our measurements support the hypothesis of Townsend (1998) that export ratios are relatively high over the upper 50 m in the southwestern Gulf of Maine. This leads to the next question, however, of how nutrients are made available to support the measured POC export rates. As suggested by Townsend (1998), one such mechanism

is water column nitrification within the Gulf of Maine followed by diffusion into surface waters. However, it is not clear whether diffusion alone is large enough to support the required flux of nutrients into the upper waters. One way to further examine this problem would be to investigate the magnitude of vertical eddy diffusivity using ^{7}Be.

Several researchers have demonstrated that ^{7}Be, a weakly particle reactive nuclide can be used to estimate the apparent vertical eddy diffusivity (K_z) (Silker, 1972; Young and Silker, 1974; Lee et al., 1991). This technique proves particularly useful in that ^{7}Be integrates the net rate of vertical mixing over several months, given its relatively long half-life of 53.3 d. Previous measurements conducted by Silker (1972) and Young and Silker (1974) have found vertical eddy diffusivities on the order of 0.1–0.9 cm^2 s^{-1} at depths of 30–60 m in waters west of California and east of Barbados. In comparison, Lee et al. (1991) have found vertical eddy diffusivities to be an order of magnitude greater, >7 cm^2 s^{-1}, in near-shore sites off the coast of California. In the Gulf of Maine, a wide range of K_z's have been estimated depending on the area and season (0.3–4 cm^2 s^{-1}: Townsend, 1992). Methods of determining K_z within the Gulf are varied and include those derived from empirical models to extrapolation from areas of similar physical processes (Garside, 1985; Loder and Platt, 1985; Townsend, 1992).

The predominant method for determination of K_z using ^{7}Be is based on the steady-state model first described by Silker (1972). If the input from rain is constant and the radionuclides are not removed by particle settling, the radionuclide concentration as a function of depth can be characterized by

$$C_2 = C_1 \exp[-z(\lambda/K_z)^{0.5}] \tag{4}$$

where C_1 and C_2 are the measured concentrations at a depth interval, z, apart, λ is the known decay constant, and K_z is the coefficient of vertical eddy diffusion. It should be noted that this model predicts that there are gradients in ^{7}Be activities with depth. As a result, vertical eddy diffusivities were determined only for the two summer cruises, July and August, due to an inability to sample below the mixed layer during cruises in the spring.

Measurements of atmospheric deposition of ^{7}Be were made several weeks prior to and during each cruise at Woods Hole, MA (south of the study area: 41°32′ N, 70°39′ W) and Portsmouth, NH (west of the sampling site: 43°04′ N, 70°42′ W) (Benitez-Nelson and Buesseler, 1999a). The average flux between these sites was used to evaluate the seasonal fluctuation in ^{7}Be deposition at Wilkinson Basin. The average ^{7}Be flux was remarkably constant prior to and during the July and August cruises. Total expected ^{7}Be inventories averaged 11,640 $\pm$ 118 d.p.m. m^{-2}, matching within error measured ^{7}Be inventories of 11,220 $\pm$ 1930 and 11,906 $\pm$ 1890 d.p.m. m^{-2} for July and August, respectively.

Our measurements of ^{7}Be in the Gulf of Maine show typically less than 10% of the total ^{7}Be activity was on particulate material and there were no clear seasonal or spatial trends (Table 1, Fig. 2). Such patterns would be expected if a significant fraction of ^{7}Be was removed on settling particulate material (e.g. ^{234}Th). Small

offshore and alongshore gradients in ^{7}Be activity suggest that horizontal advection and diffusion of ^{7}Be is small.

An additional check on the particulate removal of ^{7}Be was determined using ^{234}Th. The flux of ^{7}Be out of the upper 50 m can be determined in the same manner as the flux of particulate organic carbon, by multiplying the ratio of ^{7}Be/^{234}Th by the measured SS export flux of ^{234}Th. In July, ^{7}Be particulate activities were detectable in the upper 37 m only. Thus, only the average ^{7}Be/^{234}Th ratio over the upper 37 m was used. Results indicate that 830 d.p.m. m^{-2} of ^{7}Be, less than 8% of the expected inventory, is removed on sinking particles. A similar calculation was made for August using the average particulate ^{7}Be/^{234}Th activity ratio over the upper 45 m. In August, the flux of particulate ^{7}Be was over three times greater, 2880 d.p.m. m^{-2} or 25% of the expected inventory. However, this is most likely a substantial overestimation since the particulate ^{7}Be activity in the upper 30 m was below detection and the ^{234}Th particulate activities extremely low.

Using Eq. (4), we calculated a vertical eddy diffusivites of 1.5 ± 0.4 cm^2 s^{-1} for July, and 0.5 ± 0.2 cm^2 s^{-1} for August for the flux of dissolved material into the upper 15 m (Figs. 3 and 5). Although uncertainties are large, ^{7}Be provides a good estimate of the apparent vertical eddy diffusivity integrated over the mean life of ^{7}Be (76 d). Using this information coupled with vertical gradients of NO$_3$ + NO$_2$, we calculated that the 'new' nitrogen flux into the upper 10 m of the water column was 1.4 and 0.2 mmol N m^{-2} d^{-1} for July and August, respectively. Assuming an RKR ratio of 6.6, the flux of new nitrogen was sufficient, within errors, to support the 10 m integrated particulate organic carbon export flux of 4.7 ± 1.5 and 1.6 ± 0.7 mmol C m^{-2} d^{-1} which occurred during the July and August cruises.

The ^{7}Be model assumes steady-state and, unfortunately, ignores the cycle of mixed layer shoaling and deepening, which occurs throughout the seasons. Thus, vertical eddy diffusion rates derived from Eq. (4) can be substantially overestimated during the spring and early summer (Kadko and Olson, 1998). However, this effect would only be expected to be important for the July cruise, when shoaling of the mixed layer in early May sequesters dissolved ^{7}Be below the mixed layer. The depth of the mixed layer does not change between the July and August cruises (Fig. 3). Given the low calculated K_z values and the time interval between the development of the summer mixed layer and subsequent ^{7}Be measurement, it would appear that the effect of mixed layer shoaling was small.

Our measurements of vertical eddy diffusivity are similar to the estimates of 0.3 cm^2 s^{-1} found previously in Wilkinson Basin during the stratified summer and are well within the range of the 0.1–7 cm^2 s^{-1} found in other areas of the Gulf of Maine and in different coastal regimes (e.g. Lee et al., 1991; Townsend, 1992). It should be noted that the previous vertical eddy diffusivity estimates found for Wilkinson Basin were determined in a completely different manner, by using an empirical relationship based on temperature (e.g. King and Devol, 1979). In contrast, our estimates of the 'new' nitrogen flux into the upper 10 m are over 50% less than those determined by Townsend (1992). The discrepancy is most likely due to differences in the chosen depth interval of interest as well as real differences

between $NO_3 + NO_2$ profiles. Nonetheless, our measurements of vertical eddy diffusivity provide additional evidence that upward diffusion of nitrogen is adequate to support the measured organic carbon export from the upper 10 m in central Wilkinson Basin.

5. Conclusion

Our measurements provide some of the first direct estimates of particulate organic carbon export in the southwestern Gulf of Maine. Carbon export rates varied both seasonally and spatially. Fluxes tended to be largest nearshore and decreased with increasing distance from land, indicating the importance of the coast on [234]Th activity distributions. In March, high particulate export occurred during the spring phytoplankton bloom, whereas high rates in August were most likely the result of zooplankton grazing and fecal pellet production. The average annual export ranged between 6.2 and 14.4 mmol C m^{-2} d^{-1}, depending on the depth of integration. The average export ratio, based on primary productivity measurements of O'Reilly and Busch (1984) and Charette et al. (2000), ranged between 9 and 49%, similar to that found in many coastal environments. Accurate determinations of surface [234]Th derived particulate export, however, necessitated the inclusion of both NSS and horizontal mixing. Omission of these processes generally resulted in substantial over predictions of particulate organic carbon export. Our study provides additional support for the incorporation of such processes in using [234]Th in coastal regimes.

In contrast to [234]Th, our measurements of the weakly particle reactive radionuclide [7]Be, showed no seasonality in its distribution and only minor offshore gradients in activity. Vertical eddy diffusion rates into the upper 15 m of the water column were 1.5 and 0.5 cm^2 s^{-1}. These estimates coupled with $NO_3 + NO_2$ profiles suggest that the transport of 'new' nitrogen into surface waters was sufficient to support the export flux of particulate organic carbon. Thus, as initially suggested by Townsend (1998), nitrification followed by upwards diffusion is a viable mechanism by which high organic carbon export rates can be maintained.

Acknowledgements

References

Barrick, R.C., Prahl, F.G., 1987. Hydrocarbon geochemistry of the Puget Sound Region-III. Polycyclic aromatic hydrocarbons in sediments. Estuarine Coastal and Shelf Science 25, 175–191.

Bacon, M.P., Cochran, J.K., Hirschberg, D., Hammar, T.R., Fleer, A.P., 1996. Export flux of carbon at the equator during the EqPac. time-series cruises estimated from ^{234}Th measurements. Deep-Sea Research II 43, 1133–1154.

Benitez-Nelson, C.R., Buesseler, K.O., 1999a. ^{32}P, ^{33}P, ^{7}Be, and ^{210}Pb: Atmospheric fluxes and utility in tracing Stratosphere/Troposphere exchange. Journal of Geophysical Research 104, 11745–11754.

Benitez-Nelson, C.R., Buesseler, K.O., 1999b. Variability of inorganic and organic phosphorus turnover rates in the coastal ocean. Nature 398, 502–505.

Bigelow, H.B., 1926a. Plankton of the offshore waters of the Gulf of Maine. Bulletin of the Bureau of Fisheries, United States 40, 1–509.

Bigelow, H.B., 1926b. Physical oceanography of the Gulf of Maine. Bulletin of the Bureau of Fisheries, United States 40, 511–1027.

Brooks, D.A., 1985. Vernal circulation in the Gulf of Maine. Journal of Geophysical Research 90, 4687–4705.

Brooks, D.A., 1991. A brief overview of the physical oceanography of the Gulf of Maine. In: Wiggen, T., Mooers, C.N.K. (Eds.), Proceedings of the Gulf of Maine Scientific Workshop, Woods Hole, pp. 51–74.

Buesseler, K.O., 1998. The decoupling of production and particle export in the surface ocean. Global Biogeochemical Cycles 12, 297–310.

Buesseler, K.O., Bacon, M.P., Cochran, J.K., Livingston, H.D., 1992a. Carbon and nitrogen export during the JGOFS North Atlantic Bloom Experiment estimated from ^{234}Th:^{238}U disequilibria. Deep-Sea Research 39, 1115–1137.

Buesseler, K.O., Cochran, J.K., Bacon, M.P., Livingston, H.D., Casso, S.A., Hirschberg, D., Hartman, M.C., Fleer, A.P., 1992b. Determination of thorium isotopes in seawater by non-destructive and radiochemical procedures. Deep-Sea Research 39, 1103–1114.

Buesseler, K.O., Michaels, A.F., Seigel, D.A., Knap, A.H., 1994. A three-dimensional time-dependent approach to calibrating sediment trap fluxes. Global Biogeochemical Cycles 8, 179–193.

Buesseler, K.O., Andrews, J.A., Hartman, M.C., Belastock, R., Chai, F., 1995. Regional estimates of the export flux of particulate organic carbon derived from thorium-234 during the JGOFS EQPAC program. Deep-Sea Research II 42, 777–804.

Buesseler, K.O., Ball, L., Andrews, J., Benitez-Nelson, C., Belastock, R., Chai, F., Chao, Y., 1998. Upper ocean export of particulate organic carbon in the Arabian Sea derived from Thorium-234. Deep-sea Research II 45, 2461–2487.

Campbell, D.E., 1986. Process variability in the Gulf of Maine — a macroestuarine environment. In: Wolfe, D.A. (Ed.), Estuarine Variability. Academic Press, New York, pp. 261–275.

Charette, M.A., Moran S.B., Pilskaln, C.H. 1996. Particulate organic carbon export fluxes in the central Gulf of Maine estimated from ^{234}Th/^{238}U disequilibria. Poster presented at the Gulf of Maine Ecosystem Dynamics: A Scientific Symposium and Workshop, St. Andrews, NB, September.

Charette, M.A., Moran, S.B., Pike, S.M., Smith, J.N., 2000. Investigating the carbon cycle in the Gulf of Maine using the natural tracer thorium-234. Journal of Geophysical Research-Oceans, submitted.

Chen, J.H., Edwards, R.L., Wasserburg, G.J., 1986. ^{238}U, ^{234}U and ^{232}Th in seawater. Earth and Planetary Science Letters 80, 241–251.

Christensen, J.P., Smith, D.B., Mayer, L.M., 1991. The nitrogen budget of the Gulf of Maine and climate change. In: Wiggen, T., Mooers, C.N.K., (Eds.), Proceedings of the Gulf of Maine Scientific Workshop, Woods Hole, pp. 75–90.

Coale, K.H., Bruland, K.W., 1985. ^{234}Th: ^{238}U disequilibria within the California current. Limnology and Oceanography 30, 22–33.

Coale, K.H., Bruland, K.W., 1987. Ocean stratified euphotic zone as elucidated by ^{234}Th:^{238}U disequilibria. Limnology and Oceanography 32, 189–200.

Cochran, J.K., Barnes, C., Achman, D., 1995. Thorium-234/Uranium-238 disequilibrium as an indicator of scavenging rates and particulate organic carbon fluxes in the northeast polynya, Greenland. Journal of Geophysical Research 100, 4399–4410.

Cochran, J.K., Roberts, K.A., Barnes, C., Achman, D., 1997. Radionuclides as indicators of particle and carbon dynamics on the East Greenland Shelf. In: Germain, P. et al., (Eds.), Radioprotection-colloques, 32(C2), Proceedings of RADOC 96–97 'Radionuclides in the Oceans', pp. 129–136, Institute de Protection et de Surete nucleaire, Cherbourg, France.

Durbin, E.G., Durbin, A.G., Beardsley, R.C., 1995. Springtime nutrient and chlorophyll *a* concentrations in the southwestern Gulf of Maine. Continental Shelf Research 15, 433–450.

Eppley, R.W., Peterson, B.J., 1978. Particulate organic matter flux and planktonic new production in the deep ocean. Nature 282, 677–680.

Fitzwater, S.E., Knauer, G.A., Martin, J.H., 1982. Metal contamination and its effect on primary production measurements. Limnology and Oceanography 27, 544–551.

Garside, C., 1985. The vertical distribution of nitrate in open ocean surface water. Deep Sea Research 32, 723–732.

Gottlieb, E.S., Brooks, D.A., 1986. Current meter and atmospheric data from the Gulf of Maine: 1982–1985. Technical Report 86-3-T, Texas A&M University, 80 pp.

Gran, H.H., Braaurd, T., 1935. A quantitative study of the phytoplankton in the Bay of Fundy and the Gulf of Maine (including observations on hydrography, chemistry, and turbidity). Journal of the Biological Board of Canada 1, 279–467.

Gunderson, K., Michaels, A., Bates, N., 1993. Determination of particulate organic carbon and nitrogen. In: Bats Method Manual Version 3. Bermuda Biological Station for Research, Inc., Bermuda, 108 pp.

Gustafsson, Ö., Buesseler, K.O., Rockwell Geyer, W., Bradley Moran, S., Gschwend, P.M., 1998. On the relative significance of horizontal and vertical transport of Chemicals in the Coastal Ocean: Application of a Two-Dimensional Th-234 cycling model. Continental Shelf Research 18, 805–829.

Kadko, D., Olson, D., 1998. Be-7 as a tracer of surface water subduction and mixed layer history. Deep-Sea Research I 43, 89–116.

Kaufman, A., Li, Y.-H., Turekian, K.K., 1981. The removal rates of ^{234}Th and ^{228}Th from waters of the New York Bight. Earth and Planetary Science Letters 54, 385–392.

Kennicutt II, M.C., Wade, T.R., Presley, B.J., Requejo, A.G., Brooks, J.M., Denoux, G.J., 1994. Sediment contaminants in Casco Bay, Maine: Inventories, sources, and potential for biological impact. Environmental Science Technology 28, 1–15.

King, F.D., Devol, A.H., 1979. Estimates of vertical eddy diffusion through the thermocline from phytoplankton nitrate uptake rates in the mixed layer of the eastern tropical Pacific. Limnology and Oceanography 24, 645–651.

Larsen, P.F., Gadbois, D.F., Johnson, A.C., 1985. Observations on the distribution of PCBs in the deep water sediments of the Gulf of Maine. Marine Pollution Bulletin 16, 439–442.

Lee, T., Barg, E., Lal, D., 1991. Studies of vertical mixing in the Southern California Bight with cosmogenic radionuclides ^{32}P and ^{7}Be. Limnology and Oceanography 36, 1044–1053.

Loder, J.W., Platt, T., 1985. Physical controls on phytoplankton production at tidal fronts. In: Gibbs, P.E. (Ed.), Proceedings of the Nineteenth European Marine Biology Symposium, Cambridge Univ. Press, Cambridge, 541 pp.

Luo, S., Ku, T.-L., Kusakabe, M., Bishop, J.K.B., Yang, Y.-L., 1995. Tracing particle cycling in the upper ocean with ^{230}Th and ^{228}Th – An investigation in the equatorial Pacific along 140°W. Deep-Sea Research 42, 805–829.

McKee, B.A., DeMaster, D.J., Nittrouer, C.A., 1984. The use of ^{234}Th/^{238}U disequilibrium to examine the fate of particle-reactive species on the Yangzee continental shelf. Earth and Planetary Science Letters 68, 431–442.

Meise, C.J., O'Reilly, J.E., 1996. Spatial and seasonal patterns in abundance and age-composition of *Calanus finmarchicus* in the Gulf of Maine and on Georges Bank: 1977–1987. Deep-Sea Research II 43, 1473–1501.

Moran, S.B., Buesseler, K.O., 1993. Size-fractionated [234]Th in Continental Shelf Waters off New England: implications for the role of colloids in oceanic trace metal scavenging. Journal of Marine Research 51, 893–922.

Moran, S.B, Charette, M.A., Pike, S.M., Wicklund, C.A., 2000. Difference in seawater particulate organic carbon concentration in samples collected using small-volume and large-volume methods: the importance of DOC adsorption to the filter blank Marine Chemistry, accepted.

Murray, J.W., Downs, J.N., Strom, S., Wei, C.-L., Jannasch, W.H., 1989. Nutrient assimilation, export production and [234]Th scavenging in the eastern equatorial Pacific. Deep-Sea Research I 36, 1471–1489.

Murray, J.W., Young, J., Newton, J., Dunne, J., Chapin, T., Paul, B., McCarthy, J.J., 1996. Export flux of particulate organic carbon from the central equatorial pacific determined using a combined drifted trap-[234]Th approach. Deep-Sea Research II 43, 1095–1132.

Naimie, C., 1996. Georges Bank residual circulation during weak and strong stratification periods: prognostic numerical model results. Journal of Geophysical Research 101, 6469–6486.

Okubo, A., 1971. Oceanic diffusion diagrams. Deep-Sea Research 18, 789–802.

O'Reilly, J.E., Busch, D.A., 1984. Phytoplankton primary production on the northwestern Atlantic Shelf. Rapport P.-v. Reun. Cons. Int. Explor. Mer. Vol. 183, pp. 255–268.

Peltzer, E.T., Hayward, N.A., 1996. Spatial and temporal variability of total organic carbon along 140°W in the equatorial Pacific Ocean in 1992. Deep-Sea Research II 43, 155–1180.

Pilskaln, C.H., Lehmann, C., 1998. Seasonal biogeochemical particle fluxes and sediment resuspension processes in the coastal sea: the Gulf of Maine. The Oceanography Society, Paris.

Pollard, C., Battisto, G., Keese E., Rutan, B.J., 1996. Analytical service center procedure summaries. Virginia Institute of Marine Science/School of Marine Science, College of William and Mary, Gloucester Point, VA, February, 35 pp.

Santchi, P.H., Li, Y.-H., Bell, J., 1979. Natural radionuclides in the water of Narragansett Bay. Earth and Planetary Science Letters 45, 201–213.

Schlitz, R.J., Cohen, E.B., 1984. A nitrogen budget for the Gulf of Maine and Georges Bank. Biology Oceanography 3, 203–221.

Silker, W.B., 1972. Horizontal and vertical distributions of radionuclides in the north Pacific Ocean. Journal of Geophysical Research 77, 1061–1070.

Sverdrup, H.U., 1953. On condition of vernal blooming of phytoplankton. Journal du Counseil p.l'Exploration de la Mer 18, 287–295.

Tanaka, N., Takeda, Y., Tsunogai, S., 1983. Biological effect on removal of Th-234, Po-210 and Pb-210 from surface water in Funka Bay, Japan. Geochimica et Cosmochimica Acta 47, 1783–1790.

Townsend, D.W., 1991. Influences of oceanographic processes on the biological productivity of the Gulf of Maine. Review of Aquatic Sciences 4, 1–20.

Townsend, D.W., 1992. An overview of oceanography and biological productivity in the Gulf of Maine. The Gulf of Maine–NOAA Coastal Ocean Program Regional Synthesis Series 1, 5–26.

Townsend, D.W., 1998. Sources and cycling of nitrogen in the Gulf of Maine. Journal of Marine Systems 16, 283–295.

Townsend, D.W., Spinrad, R.W., 1986. Early spring phytoplankton blooms in the Gulf of Maine. Continental Shelf Research 6, 515–529.

US JGOFS Planning Report 11, 1990. U.S. Joint Global Ocean Flux Study Long Range Plan, The Role of Biogeochemical Cycles in Climate Change, U.S. JGOFS Steering Committee. US JGOFS Planning Office, Woods Hole, MA, 216 pp.

Vermersch, J.A., Beardsley, R.C., Brown, W.S., 1979. Winter circulation in the Western Gulf of Maine: Part 2. Current and pressure Observations. Journal of Physical Oceanography 9, 768–784.

Walsh, J.J., Whitledge, T.E., O'Reilly, J.E., Phoel, W.C., Draxler, A.E., 1987. Nitrogen cycling on Georges Bank and the New York Shelf: comparison between well-mixed and seasonally stratified waters. In: Backus, R.H. (Ed.), Georges Bank. MIT Press, Cambridge, pp. 234–246.

Wageman, R., Muir, D.C.G., 1984. Concentrations of heavy metals and organochlorides in marine mammals of northern waters: Overview and evaluation. Canadian Technical Report Fisheries Aquatic Science No. 1279, p. 97.

Wei, C.-L., Murray, J.W., 1992. Temporal variations of ^{234}Th activity in the water column of Dabob Bay: Particle scavenging. Limnology and Oceanography 37, 296–314.

Young, J.A., Silker, W.B., 1974. The determination of air–sea exchange and oceanic mixing rates using ^{7}Be during the bomex experiment. Journal of Geophysical Research 79, 4481–4489.

Zapata, M., Ayala, A.M., Franco, J.M., Garrido, J.L., 1987. Separation of chlorophylls and their degradation products in marine phytoplankton by reversed-phase high performance liquid chromotography. Chromotographia 23, 26–30.